International Journal of Thermofluid Science and Technology (2023)
Volume 10, Issue 2, Paper No. 100203
https://doi.org/10.36963/IJTST.2023100203

Research Article

Free convection of hybrid water/aluminum oxide-copper nanofluid in cubic cavity

Dayf Abdellatif[1*], Feddaoui M'barek[1], Bouchta Said[1], Hissouf Mohamed[1], El Ihssini Hossine[2]

[1] *Laboratory of Energy Engineering, Materials and Systems, National School of Applied Sciences, Ibn Zohr University, B.P. 1136, Agadir, Morocco*
[2] *Laboratory of Mechanic, Energy and Environment Process, National School of Applied Sciences, Ibn Zohr University, B.P. 1136, Agadir, Morocco*

ATICLE INFO

Received: 18 Mar. 2023.
Received in revised form:
30 May. 2023.
Accepted: 12 Jun. 2023.
Published online:
20 Jun. 2023

Keywords:
Convection
Hybrid nanofluid
Tree-dimensional
Finite Volume

ABSTRACT

Convective heat transfer is a physical phenomenon that continues to attract the interest of researchers in many fields of science and engineering. This work aims at numerically investigating the enhancement of heat transfer in a differentially heated three-dimensional cavity using a hybrid Al_2O_3-Cu-water nanofluid and Al_2O_3-water nanofluid. The partial differential equations are discretized in 3D by adopting the finite volume method and using the SIMPLEC algorithm for pressure correction. Heat transfer and fluid flow results are presented in the form of isotherms, velocity fields and mean Nusselt number. The results show that the effect of nanofluid and hybrid nanofluid on natural convection is more significant when the Rayleigh number is high. The use of hybrid nanofluid improves the heat transfer compared to nanofluid.

1. Introduction

The use of nanofluids in heat transfer by convective mode is found in various industrial processes as devices cooling, building, thermal insulation devices and power plants (Ostrach [1]). Fluids with added particles at the nanoscale are called nanofluids (Choi [2]). Several authors have studied the natural convection of nanofluids within cavities of various shapes. Heat transfer in nanofluid filled rectangular cavity in natural convection using several boundary conditions on the side walls has been conducted by Sharif and Mohammed [3]. There are a number of studies utilizing classical numerical methods to describe the free convection heat transfer in a filled enclosure cavity using nanofluid. Khanafer et al. [4] conducted a numerical study to evaluate the effect of the nanofluid on the heat transfer in a confined cavity in natural convection. The authors maintained the right and left walls as differentially heated, while the horizontal walls are supposed adiabatic. Their results indicated that the increase in volume fraction of the dispersed nanoparticles leads to enhance the heat transfer.

Oztop et al. [5] carried out a computational study of the natural convection in enclosed cavity by keeping the vertical walls at cold temperature and the horizontal walls are considered adiabatic. The air into the cavity is heated using a

Nomenclature

C_P	Specific heat at constant pressure, $(J.kg^{-1}\,K^{-1})$	μ	Dynamic viscosity$(kg.m^{-1}.s^{-1})$
g	Gravitational acceleration, $m.s^{-2}$	ϑ	Kinematic viscosity $(m^2.s^{-1})$
H	Dimension of the cubic cavity, (m)	θ	Dimensionless temperature
k	Thermal conductivity,$(W.m^{-2}\,K^{-1})$	ρ	Density $(kg.m^{-3})$
Nu	Nusselt number	φ	Volume fraction of nanoparticles
p	Pressure, (Pa)	ψ	Stream function
P	Dimensionless pressure	*Subscripts*	
Pr	Prandtl number	Avg	Average
Ra	Rayleigh number	C	Cold
T	Temperature, (K)	f	Base fluid
u, v, w	Velocity components, $(m.s^{-1})$	H	Hot
U, V, W	Dimensionless velocities	hnf	Hybrid nanofluid
x, y, z	Cartesian coordinates, (m)	hp	Hybrid particles
X, Y, Z	Dimensionless Cartesian coordinates	nf	nanofluid
Greek symbols		ref	Reference
α	Thermal diffusivity $(m^2.s^{-1})$		
β	Thermal expansion coefficient (K^{-1})		

thin plate disposed horizontally or vertically inside the cavity. The results show that there an increase in the mean Nusselt number by increasing the length of the thin plate. In addition, they observed that the location position of the plate influences on heat transfer. In fact, when the plate is located vertically the Nusselt number is improved about 20% compared to horizontally position at high Rayleigh number.

A numerical study is performed by Akhter and Mokaddes [6] to investigate to effect of the hybrid nanofluid on the heat transfer inside an enclosed cavity, with hexagonal block and an external magnetic field. The results showed that the use of the nanofluid increased the average Nusselt number by 21.85% and 40.29% in comparison to pare water for Ha=0 and Ha=100 respectively. They also shows that the presence of the magnetic field enhances the heat transfer.

Saleh et al [7] examined numerically the effect of the nanofluid on the heat transfer in a trapezoidal cavity filled with nanofluids (Water–Cu and water–Al_2O_3). They found that the suspension of Copper nanoparticles with high concentration increases significantly the feat transfer ability. Basing the obtained results, the authors have developed a correlation given the average Nusselt number in function of the heat transfer parameters.

Tric et al. [7] conducted numerically the free convection in a cubic cavity employ a pseudo-spectra Chebyshev algorithm resolution supplied by polynomial expansions. Their results indicate a non-monotonic evolution in the structure of flow when Ra increases.
Ravnik et al. [9] has been examined a free convection in a cubic cavity filled with nanofluids. The numerical approach is based on the boundary element method (BEM). They proved that nanofluids increase the heat transfer capacity in mass flows and also enhance the three-dimensional character of the flow field. Ternik [10] studied free convection of the water-Au nanofluid in a cubic cavity. The impact of the investigated fluid, nanoparticle volume fraction φ and Rayleigh number Ra on the momentum transport conditions and heat were thoroughly analyzed.

As far as natural convection of hybrid nanofluid, representing an assembly of two types of nanoparticles is concerned. Suresh et al. [11] investigated the convective heat transfer in a heated cubic cavity using Cu-Al_2O_3/water as hybrid nanofluid. At Reynolds number of 1730, the authors found that the use of Cu-

Al_2O_3/water hybrid nanofluid have a significant effect on the heat transfer enhancement in comparison to pure water. However, their results illustrate that for the same nanoparticles fraction, Cu-Al_2O_3/water hybrid nanofluids have relatively higher friction factor than Al_2O_3/water nanofluid. Hemmat et al [12] performed a study on the rheological behavior of the MWCNTs/SiO_2-SAE40 hybrid nanofluid, they experimentally established a correlation for particles of diameter 25 (Ag) and 40 (MgO) nm and a volume fraction between 0% and 2%. They noticed that this nanolubricant is acting like a Newtonian fluid for solids volume fractions of maximum 1% and as a non-Newtonian fluid for solids volume fractions between 1.5% and 2%. They also found that the kinematic viscosity reduces with the increase of the fluid temperature and increases with the nanoparticles volume fraction.

Many authors Hemmat et al. [13], Hemmat and Sarlak [14] and Kalidasan and Rajesh [15] interpreted results on the hybrid nanofluid with heaters on the vertical walls and insulated block. They indicated that increasing the percentage of nanoparticles at different Rayleigh numbers leads to drop the strength of the primary vortex.

A numerical study is conducted by Rahman et al. [16] to analyse the thermal behavior of Al_2O_3-Cu hybrid nanofluid in a two-dimensional axisymmetric copper tube. They observed that the dominant nanoparticles in the hybrid nanofluid strongly affects the thermal behavior of the hybrid nanofluid. In addition, they shown that the heat transfer coefficient enhances with the volume concentration of the hybrid nanoparticles suspended in the base fluid. Furthermore, this coefficient rises with the increase of the Reynolds number.

Ranga et al. [17] have published a review which he summarized the recent research on the synthesis, heat transfer characteristics, thermo-physical properties, hydrodynamic behavior and the flow characteristics of various hybrid nanofluids. This review also highlighted the uses and challenges of hybrid nanofluids and made some suggestions for the future research expected in this topic. Among the conclusions made by this review, the flow properties of hybrid nanofluids are refined by the suspension of hybrid nanoparticles, and their thermal conductivity is significantly higher than that of the nanofluids or base fluid.

The thermal conductivity of Ag-Al_2O_3-water is experimentally studied by Aparna et al. [18]. The impact of volume fraction of the nanoparticles as well as the mixture ratios of Ag-Al_2O_3 was analysed. They proved that the thermal conductivity has a great effect on the heat transfer as the nanoparticles volume fraction increases. The authors proposed a correlation to predict the thermal conductivity of the tested hybrid nanofluid as function of particles volume fraction and fluid temperature. Mehryan et al. [19] carried out a numerical study using hybrid nanofluid (water/ Cu-Al_2O_3) in a porous cavity. They analysed the effects of various Darcy-Rayleigh numbers and hybrid volume fraction. They indicated that the use of nanofluids caused a decrease in flow velocity and flow power. The drop is more significant for hybrid nanofluid than the nanofluid. Khalili and Sheikholeslami [20] propose a new configuration of the photovoltaic (PV) cell cooling system using a numerical approach. The cooling system contains cooling ducts of three shapes (circular, triangular and tri-lobed) and confined jets and the hybrid nanofluid. The ducts have three shapes (circular, triangular and tri-lobed). To improve the convection rate, Y-shaped fins were installed inside the ducts. The use of hybrid nanomaterials in both zones instead of water increases the useful heat and cools the cells. Regarding the different configurations, the best performance was reported for the triangular duct which has good hydrothermal performance compared to the others.

From the above literature and to the best of our knowledge, there is no studies performed on hybrid nanofluid flow in three-dimensional differentially heated cavity. The hybrid nanofluid is based on the low volume fraction of metal Cu nanoparticles. The aim of the paper is focused on the investigation of the effect of water/Cu-Al_2O_3 hybrid nanofluid on improvement of free convection fluid flow and heat transfer in a cubic cavity. A comparative study between hybrid water/Cu-Al_2O_3 and water/Al_2O_3 nanofluids is done. In addition, the

impact of Rayleigh number and solid volume fraction of hybrid nanofluid are examined.

2. Mathematical modelling

In this work a three-dimensional numerical study on the natural convective flow into a cubic cavity filled with water/Al_2O_3 nanofluid or water/Cu-Al_2O_3 hybrid nanofluid is conducted. Fig.1 represents the physical model of the cavity with the reference axes considered. The left and right walls are supposed as imposed temperature with T_H and T_C respectively. The others are assumed to be insulated walls. The suspended nanoparticles (Al_2O_3 and Cu) are considered as spherical shape and small size.

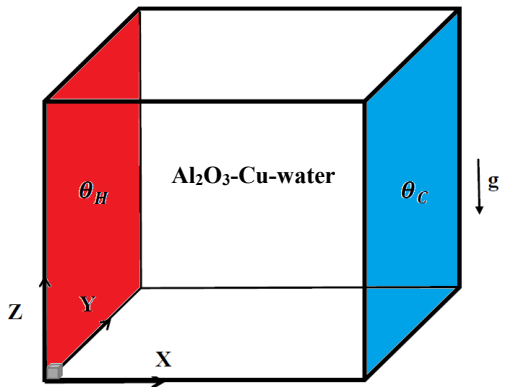

Fig. 1. Schema representing the differentially heated cavity.

In order to simplify the computational study, the following assumptions are considered:

- The flow is regular, Newtonian, laminar and incompressible.
- The nanoparticles are supposed as uniform size and shape.
- The base liquid and nanoparticles are considered homogeneous mixture, then single monophasic model is adopted.
- Except the density, the thermophysicals properties of the hybrid nanofluid and nanofluid are supposed to be constant. In fact, the density is varied according to Boussinesq approximation.

Governing Equations

$$\frac{\partial u}{\partial x}+\frac{\partial v}{\partial y}+\frac{\partial w}{\partial z}=0 \quad (1)$$

$$\rho_{hnf}\left(u\frac{\partial u}{\partial x}+v\frac{\partial u}{\partial y}+w\frac{\partial u}{\partial z}\right)=-\frac{\partial p}{\partial x}+\mu_{hnf}\left(\frac{\partial^2 u}{\partial x^2}+\frac{\partial^2 u}{\partial y^2}+\frac{\partial^2 u}{\partial z^2}\right) \quad (2)$$

$$\rho_{hnf}\left(u\frac{\partial v}{\partial x}+v\frac{\partial v}{\partial y}+w\frac{\partial v}{\partial z}\right)=-\frac{\partial p}{\partial y}+\mu_{hnf}\left(\frac{\partial^2 v}{\partial x^2}+\frac{\partial^2 v}{\partial y^2}+\frac{\partial^2 v}{\partial z^2}\right) \quad (3)$$

$$\rho_{hnf}\left(u\frac{\partial w}{\partial x}+v\frac{\partial w}{\partial y}+w\frac{\partial w}{\partial z}\right)=-\frac{\partial p}{\partial z}+\mu_{hnf}\left(\frac{\partial^2 w}{\partial x^2}+\frac{\partial^2 w}{\partial y^2}+\frac{\partial^2 w}{\partial z^2}\right)+(\rho\beta)_{hnf}g(T-T_{réf}) \quad (4)$$

$$u\frac{\partial T}{\partial x}+v\frac{\partial T}{\partial y}+w\frac{\partial T}{\partial z}=\alpha_{hnf}\left(\frac{\partial^2 T}{\partial x^2}+\frac{\partial^2 T}{\partial y^2}+\frac{\partial^2 T}{\partial z^2}\right) \quad (5)$$

In the terms of the following dimensionless variables :

$$X=\frac{x}{H},Y=\frac{y}{H},Z=\frac{z}{H},U=\frac{uH}{\alpha_f},V=\frac{vH}{\alpha_f},$$
$$W=\frac{wH}{\alpha_f},\quad P=\frac{pH^2}{\rho_{hnf}\alpha_f^2} \quad (6)$$
$$\theta=\frac{T-T_{ref}}{T_H-T_C}\ \text{Where}\ T_{ref}=\frac{T_C+T_H}{2}$$

The continuity (equation 1), momentum (equation 2-4), and energy equations (equation 5) for the considered nanofluid filled into the cavity in steady-state are written in dimensionless form as follows [10]:

$$\frac{\partial U}{\partial X}+\frac{\partial V}{\partial Y}+\frac{\partial W}{\partial Z}=0 \quad (7)$$

$$U\frac{\partial U}{\partial X}+V\frac{\partial U}{\partial Y}+W\frac{\partial U}{\partial Z}=-\frac{\partial P}{\partial X}+\frac{\mu_{hnf}}{\rho_{hnf}\alpha_f}\nabla^2 U \quad (8)$$

$$U\frac{\partial V}{\partial X}+V\frac{\partial V}{\partial Y}+W\frac{\partial V}{\partial Z}=-\frac{\partial P}{\partial Y}+\frac{\mu_{hnf}}{\rho_{nf}\alpha_f}\nabla^2 V \quad (9)$$

$$U\frac{\partial W}{\partial X}+V\frac{\partial W}{\partial Y}+W\frac{\partial W}{\partial Z}=-\frac{\partial P}{\partial Z}+\frac{\mu_{hnf}}{\rho_{hnf}\alpha_f}\nabla^2 W+\frac{(\rho\beta)_{hnf}}{\rho_{hnf}\beta_f}Ra.Pr.\theta \quad (10)$$

$$U\frac{\partial \theta}{\partial Y}+V\frac{\partial \theta}{\partial Y}+W\frac{\partial \theta}{\partial Z}=\frac{\alpha_{hnf}}{\alpha_f}\nabla^2\theta \quad (11)$$

The Prandtl number Pr and the Rayleigh number Ra are expressed as below:

$$Ra=\frac{g\beta_f H^3(T_H-T_C)}{\vartheta_f\alpha_f},\qquad Pr=\frac{\vartheta_f}{\alpha_f} \quad (12)$$

We also define the stream function ψ, represented in a plane and related to the velocity, as follows:

$$V = \frac{\partial \psi}{\partial X} \quad \text{and} \quad U = -\frac{\partial \psi}{\partial Y} \qquad (13)$$

The Table 1 summarized the thermophysical properties of the hybrid nanofluid (water/Cu-Al_2O_3) and nanofluid (water/Al_2O_3) as function of the base liquid properties and volume fraction of Al_2O_3 and Cu dispersed in the base liquid (Abu-Nada and Oztop [19]). The hybrid nanoparticle is given by considering 50% of each component, then the volume fraction of hybrid nanofluid is: $\varphi_{hp} = \varphi_{Al_2O_3} + \varphi_{Cu}$. Table 2 presents the thermophysical properties of water as well as the two nanoparticles evaluated at 25°C.

Table 1 Thermal and physical properties of the nanofluid and hybrid nanofluid.

Properties	Nanofluid (Abu-Nada and Oztop [21]	Hybrid nanofluid (Takbi and shokouhmand [22])
Density	$\rho_{nf} = (1-\varphi_p)\rho_f + \varphi\rho_p$	$\rho_{hnf} = (1-\varphi_{hp})\rho_f + \varphi_{Al_2O_3}\rho_{Al_2O_3} + \varphi_{Cu}\rho_{Cu}$
Heat capacity	$(\rho c_p)_{nf} = (1-\varphi_p)(\rho c_p)_f + \varphi(\rho c_p)_p$	$(\rho c_p)_{hnf} = (1-\varphi_{hp})(\rho c_p)_f + \varphi_{Al_2O_3}(\rho c_p)_{Al_2O_3} + \varphi_{Cu}(\rho c_p)_{Cu}$
Thermal expansion coefficient	$(\rho\beta)_{nf} = (1-\varphi_p)(\rho\beta)_f + \varphi(\rho\beta)_p$	$(\rho\beta)_{hnf} = (1-\varphi_{hp})(\rho\beta)_f + \varphi_{Al_2O_3}(\rho\beta)_{Al_2O_3} + \varphi_{Cu}(\rho\beta)_{Cu}$
viscosity	$\mu_{nf} = \frac{\mu_f}{(1-\varphi_p)^{2.5}}$	$\mu_{hnf} = \frac{\mu_f}{(1-\varphi_{hp})^{2.5}}$
Thermal conductivity	$\frac{k_{nf}}{k_f} = \frac{k_p + 2k_f - 2\varphi_p(k_f - k_p)}{k_p + 2k_f + \varphi_p(k_f - k_p)}$	$\frac{k_{hnf}}{k_f} = \frac{\frac{\varphi_{Al_2O_3}k_{Al_2O_3}+\varphi_{Cu}k_{Cu}}{\varphi_{hp}} + 2k_f + 2(\varphi_{Al_2O_3}k_{Al_2O_3} + \varphi_{Cu}k_{Cu}) - 2\varphi_{hp}}{\frac{\varphi_{Al_2O_3}k_{Al_2O_3}+\varphi_{Cu}k_{Cu}}{\varphi_{hp}} + 2k_f - (\varphi_{Al_2O_3}k_{Al_2O_3} + \varphi_{Cu}k_{Cu}) + \varphi_{hp}}$
Thermal diffusivity	$\alpha_{nf} = \frac{k_{nf}}{(\rho c_p)_{nf}}$	$\alpha_{hnf} = \frac{k_{hnf}}{(\rho c_p)_{hnf}}$

Table 2 Thermal and physical Properties of nanoparticles and water at 298.15K. [23]

Physical Properties	Water	Al_2O_3	Cu
$\boldsymbol{\mu \times 10^{-3}}$*(kg/m. s)*	8.9	-	-
$\boldsymbol{\rho(kg/m^3)}$	997.1	3970	8933
$\boldsymbol{C_P(J/kg.K)}$	4179	765	385
k (W/(m.K))	0.613	40	401
$\boldsymbol{\beta \times 10^{-5}(1/K)}$	21	0.85	1.67
$\boldsymbol{\alpha \times 10^{-7}(m^2/s)}$	1.47	131.7	1163.1

The boundary conditions relating to Eqs. (7) to (11) are as follows:

U=V=W=0, on all the walls (14)

$\theta = 1$ for X=0 (15)

$\theta = 0$ for X=1 (16)

$\frac{\partial \theta}{\partial Y} = 0$ for Y=0 and Y=1 (17)

$\frac{\partial \theta}{\partial Z} = 0$ for Z=0 and Z=1 (18)

The heat transfer in the nanofluid and hybrid nanofluid depends on the flow configuration and various properties; heat capacity, thermal conductivity of pure fluid and nanoparticles, volume fraction and viscosity. To compare the effectiveness of nanofluid (Al_2O_3-water) and hybrid nanofluid (Al_2O_3-Cu-Water) to heat transfer, the local Nusselt number and the average Nusselt number are evaluated which are expressed as:

$$Nu = -\frac{k_{nf}}{k_f}\left(\frac{\partial \theta}{\partial X}\right)_{X=0} \qquad (19)$$

$$Nu_{avg} = \int_0^1 \int_0^1 Nu_l dZdY \qquad (20)$$

In the case of hybrid nanofluid, k_{nf} will be replaced by the thermal conductivity of hybrid nanofluid k_{hnf}.

3. Numerical Approach

The finite volume method (Patankar [24]) is used to linearize the governing equations (equtions:7-11). The obtained discretized algebraic equations are then converted to a tridiagonal matrix system. The solution is based on the TDMA algorithm. The velocity-pressure coupling problem is treated using the SIMPLEC algorithm. A numerical code is built in FORTRAN language. The solution is obtained by solving the linearized equations line by line. The convergence criteria of the numerical model is based on the calculate of absolute normalized residuals of the equations that have been summed for all cells of the computational domain (Hoffman [25]). The flowchart describing the numerical resolution steps is presented in the Fig.2.

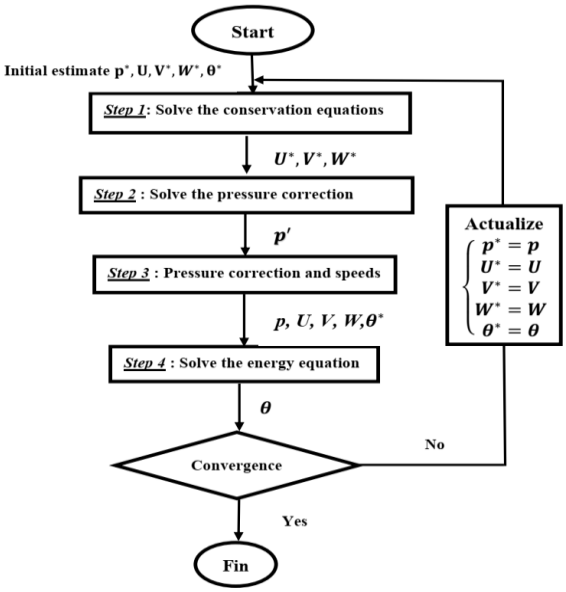

Fig.2. Sequence of steps in the SIMPLEC flowchart.

To check the grid independence to numerical solution, five grids generated with different sizes are tested. Uniform grid is chosen in all directions as depicted in the Figure 2. For an optimum solution between results precision and time of the system resolution (Table 3), the grid 61×61×61 is kept in this study.

To validate our computational study, the

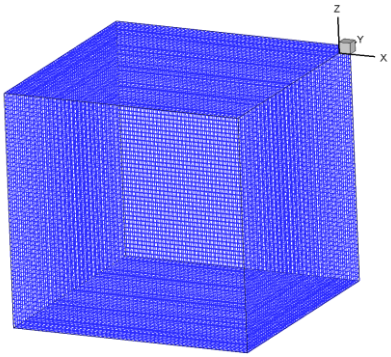

Fig. 3. Generated grid in the three direction of the studied cavity.

presents obtained results are compared to literature available data; Fusegi et al. [26], Tric et al. [7], Peng et al. [27], Lo et al. [28], Ravnik et al. [8] and Ternik [9] in free convection of the air in the cubic cavity at the Rayleigh number between 10^3 to 10^6. The Table 4 summarized the data comparison between our findings and the results of the corresponding benchmark studies. As shown in the table good agreement is observed between our simulations and those reported by the previous researchers. In fact, the maximum relative error is found to be 1.12%.

Table 3 Grid sensitivity study for Ra=10^5 $\boldsymbol{\varphi_{hp} = 3\%}$ and $\boldsymbol{\varphi_{hp} = 5\%}$ hybrid nanofluid.

Grid size	Nu_{avg} for $\boldsymbol{\varphi_{hp} = 5\%}$	Relative error
$\mathbf{21 \times 21 \times 21}$	5.1119	-
$\mathbf{31 \times 31 \times 31}$	4.8796	4.67%
$\mathbf{41 \times 41 \times 41}$	4.7912	1.81%
$\mathbf{51 \times 51 \times 51}$	4.7453	0.95%
$\mathbf{61 \times 61 \times 61}$	4.7168	0.60%
$\mathbf{71 \times 71 \times 71}$	4.6965	0.07%
$\mathbf{81 \times 81 \times 81}$	4.6752	0.06%

Numerical simulations are used to study the operation and properties of modeled systems of real and often complex phenomena and to predict their evolution. If their use is generally more economical and flexible than real experiments, validations are always essential to guarantee their relevance.

Table 4 Comparison of the average Nusselt number of the air in natural convection in the cubic cavity.

Ra	10^3	10^4	10^5	10^6
Present study	1.073	2.077	4.373	8.698
Tric et al. [7]	1.070	2.054	4.337	8.641
Ravnik et al. [8]	1.071	2.056	4.343	8.679
Ternik [9]	1.071	2.049	4.327	8.627
Fusegi et al. [26]	1.085	2.100	4.361	8.770
Peng et al. [27]	1.075	2.085	4.378	----
Lo et al. [28]	1.071	2.054	4.333	8.666

The second validation concerns an experimental configuration presented by Bajorek and Lloyed [29]. The experimental setup and the approach applied to perform the measurements are presented in this reference. It consists of an air-filled cavity with or without partitions for Grashof numbers between 1.7×10^5 and 3.0×10^6 whose vertical walls are kept at constant temperature. While the other horizontal walls are adiabatic. A comparative investigation between our numerical and experimental results from Bajorek and Lloyed [27] for the air temperature profiles in the cavity is given by Fig. 4. The results show that there is a very good agreement with a relative error of less than 2.06%.

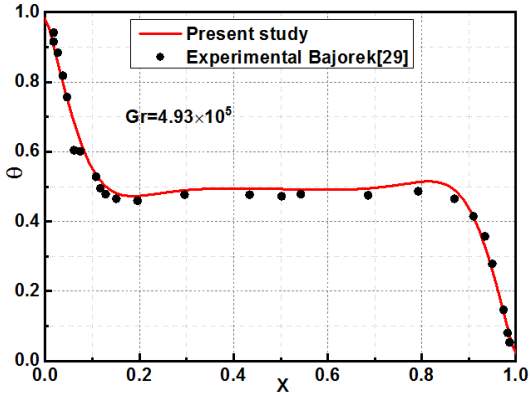

Fig. 4. Comparison of the obtained results concerning temperature profile versus experimental values of Bajorek and Lloyed [29].

4. Results and discussion

In this inquiry, free convection heat transfer in three-dimensional cubic enclosure filled with a hybrid nanofluid is numerically examined. The hybrid nanofluid Al_2O_3-Cu-water is considered with various volume fractions of Cu and Al_2O_3 nanoparticles by considering the mixture of Al_2O_3 nanoparticles and Cu-water nanofluid to form the required hybrid nanofluid $\varphi_{\mathrm{hnf}} = \varphi_{Al_2O_3} + \varphi_{\mathrm{Cu}}$ .The volume fraction taken in this work is less than 5%, and the Rayleigh number ranges from 10^3 to 10^6. Particular attention is given to hybrid nanofluid with low volume fraction of metal Cu nanoparticles.

4.1 Temperature contours

Fig. 5 illustrates the temperature contours in the central plane (a) X=0.5, (b) Y=0.5 and (c) Z=0.5. Comparing the temperature field's pure water and hybrid nanofluid (Al2O3-Cu-water), we note practically similar temperature repartition in the central part of the cavity. The difference between pure fluid (φhnf=0%) and hybrid nanofluid with φhnf=5% can be clearly seen in the dominated conduction cases (small Rayleigh number). We noted that at a smaller flow velocity, higher volume fraction displaced the temperature, contour far from the wall and hence reduced the temperature gradient. The latter is much lower than the improvement obtained at high Rayleigh number. In cases of dominating convection (high Rayleigh number), this influence is much smaller and has no major impact on total heat transfer.

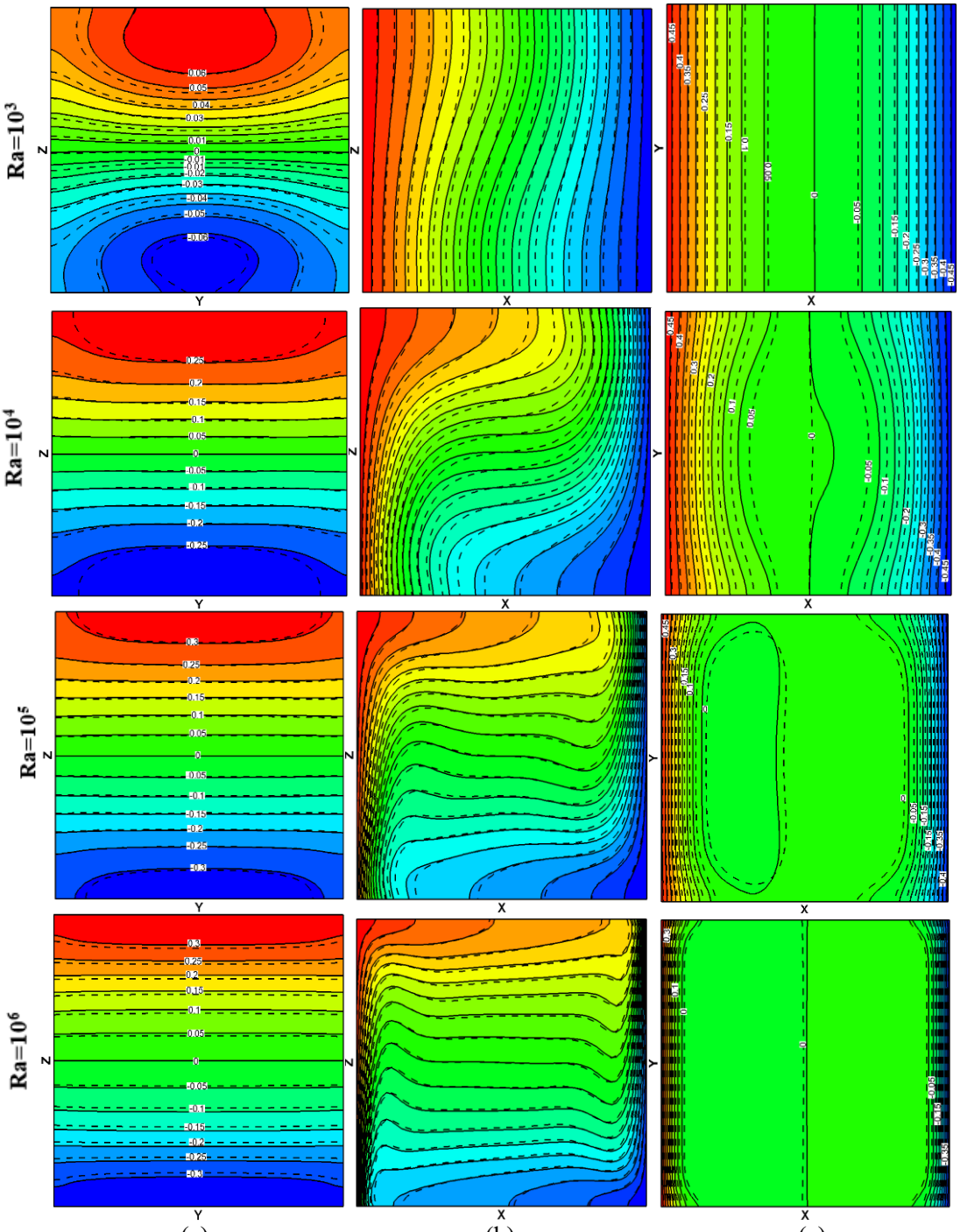

Fig. 5. Temperature contours on the central plane (a) X=0.5, (b) Y=0.5 and (c) Z=0.5, for water (—) and hybrid nanofluid (Water-Al_2O_3-Cu) (----) for different Rayleigh numbers, $\varphi_{hnf} = 5\%$.

The Fig. 6 realizes the streamlines for the hybrid nanofluid (water-Al_2O_3-Cu) in the plane Y=0.5, Ra in the range of 10^3 to 10^6 with a volume fraction $\varphi_{hnf} = 5\%$. The otained results in the case of the base fluid (water) are also plotted in the same figures in order to compare and to highlight the impact of the dispersion of the nanoparticles (Al_2O_3 and Cu) on the dynamic temperature field. It is observed that the flow structure is characterized a single cell occupying practically the entire cavity for the different values of the Rayleigh number used in this study.

The values of ψ (Stream function) increase with the rise of Rayleigh number. Thus, it is revealed that the pure fluid flow is stronger than the hybrid nanofluid flow for $Ra \leq 10^4$. The streamlines become tighter next to the side walls. However, the cells shape changes completely for flow with $Ra \geq 10^4$. The hybrid nanofluid flow then becomes the strongest. According these figures, it is found that the water and the hybrid nanofluid have approximatively the same dynamic behavior.

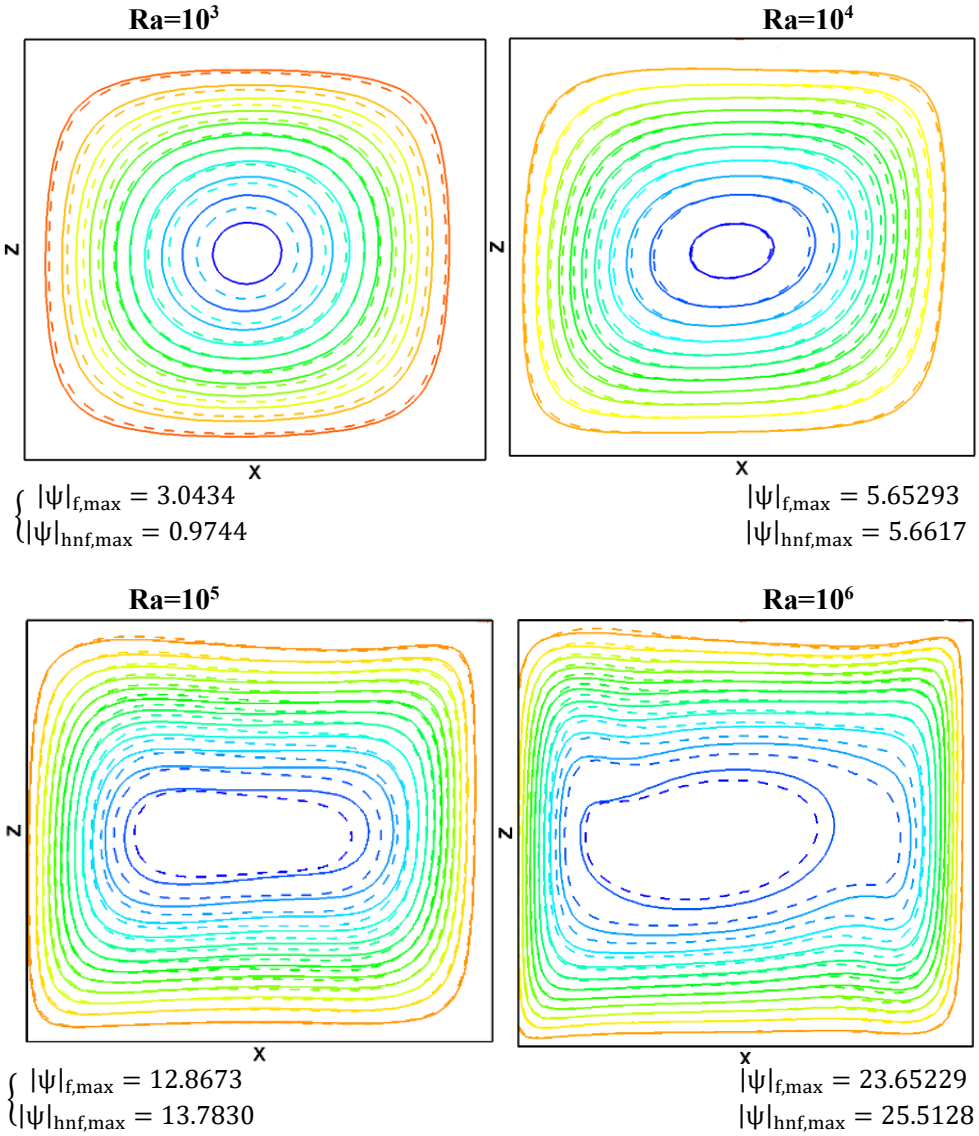

Fig. 6. Streamline for water (—) and hybrid nanofluid (Water-Al_2O_3-Cu) (----) for various Rayleigh numbers, $\varphi_{hnf} = 5\%$ plotted at the plane Y=0.5.

4.2 Velocity profiles

The variety of non-dimensional vertical velocity W and horizontal velocity U for different positions of Y, in the case of a hybrid nanofluid with Ra=10^3,10^4, 10^5 and 10^6 is presented in Fig. 7. The three-dimensional nature of the flow is apparent as there is a significant difference between the velocity profiles U and W for different Y-planes. For Ra=10^3 and 10^4, the maximum velocity is reached at Y=0.5 and between $0 < X < 0.5$ and $0 < Z < 0.5$ for the two components U and W respectively. Also, all velocity profiles indicate a null velocity located at the middle plane X = 0.5 and Z = 0.5. Because of the significant

velocity gradients observed for the small X and Z distances, the values of velocity are widely higher than those observed nigh the upper wall characterized by high X and Z values. This result is explained by that the fluid in the lower part of the main vortex must pass through a smaller region. The main role of the back wall in this case is only to decrease the magnitude of the velocity for Y = 0.05 due to viscous effects. Nevertheless, there is no notable change in the velocity profile shape. For Ra=10^5 and 10^6 significant effect of the rear walls is observed. The Fig 5 indicates that the back hot wall has a great effect on the temperature profiles especially beside the wall.

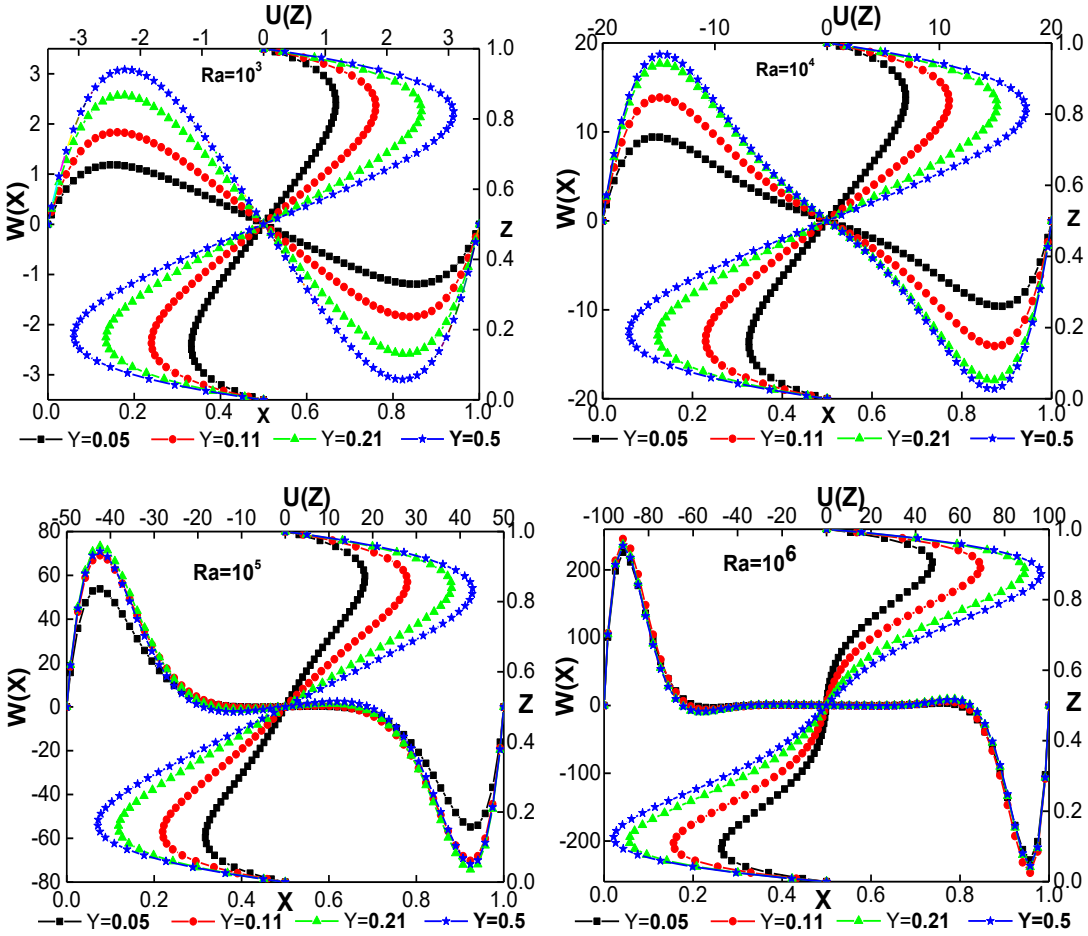

Fig. 7. Velocity profiles U (Z) and W(X) along the mid-part of the cube for various values of $\boldsymbol{Y}$ and different Ra for water/Al_2O_3-Cu hybrid nanofluid at $\boldsymbol{\varphi_{hp} = 5\%}$.

Fig. 8 presents specific profiles for of velocity U(Z) in function Z and velocity W(X) in function X for water/Al_2O_3-Cu hybrid nanofluid at mid-party of the enclosure Y = 0.5 for Ra from 10^3 to 10^6 and for three values from φ_{hp} (0%, 3% and 5%). In the case of the dominance of heat transfer by conduction (Ra = 10^3), it should be to note that the water reachs high velocities. While, the addition of the solid nanoparticles leads to retard the fluid flow. Therefore, the reduction in velocity results in a decrease in convective heat transfer effect. Nevertheless, as the thermal regime is mainly transported by conduction, the decrease caused by the low velocity is practically small and the overall heat transfer of the hybrid nanofluid is very inportant due to the great thermal conductivity of a hybrid nanofluid.

In the cases of Rayleigh number upper than Ra = 10^4, the convection is dominated. In fact, we observed that the velocities achieved by the hybrid nanofluid are higher than those of the base fluid. Therefore, the use of hybrid nanofluids increase the velocity, and as a result,

an improvement of heat transfer is obtained. The increase in heat transfer relative to the convection dominate is lawer than that of the heat conduction dominated case, which is due to the important increase in thermal conductivity as nanoprticules dispersed in the pure water.

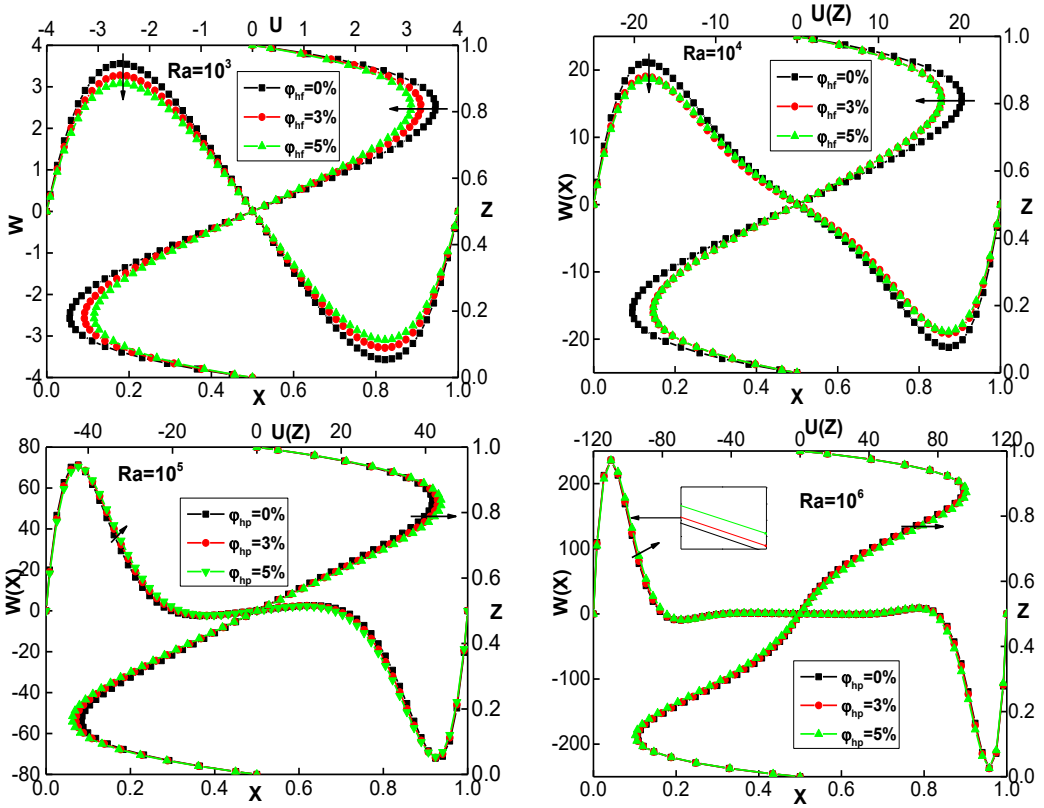

Fig. 8. Velocity profiles U (Z) and W(X) for $\boldsymbol{\varphi_{hp}} = \mathbf{0}\%, \mathbf{3}\%, \mathbf{5}\%$ and different Rayleigh number (Ra).

4.3 Nusselt Number

Quick analyses of Fig. 9 reveals that the Nusselt number local variation along the left hot wall of the cubic at the volume portion of the nanoparticles $\varphi_{hnf} = 5\%$ distinct Rayleigh numbers between pure water, water/Al_2O_3 and water/Al_2O_3-Cu. In addition, it appears from the figures at Ra = 10^3 that the enhancement is noticed with the augmentation of volume fraction of the nanoparticles for both nanofluids and hybrid nanofluids against pure water. The buoyancy force is weak with great contribution of convection in heat transfer compared to conduction. Consequently, for Ra =10^4, the rate of heat transfer rises with a larger concentration of nanoparticles.

At Ra =10^5 and Ra=10^6 the fluid flow is superior to that at Ra =10^4. It shall be noted that by raising the values of Ra, local Nusselt number raises and becomes more than ten times its value at the wall (Z =0). An improvement in heat transfer is achieved as a result of the increase in the volume fraction; consequently, the local Nusselt index for nanofluid (water/Al_2O_3), hybrid nanofluid (water/Al_2O_3-Cu) and pure water occurs at the upper end of the hot wall. The hybrid nanofluid has the highest values of the local Nusselt Index compared to traditional nanofluid and pure water.

To allow for a broader comparison, Fig. 10 illustrates the evolution of the average Nusselt numbers with volume fraction for different Ra. It can be seen that the Nu_{avg} increases linearly at higher volume fraction for both the nanofluid and hybrid nanofluid cases, revealing a better heat transfer situation. For similar volume fractions, the average Nusselt number estimates for the hybrid nanofluid are higher than those for the nanofluid.

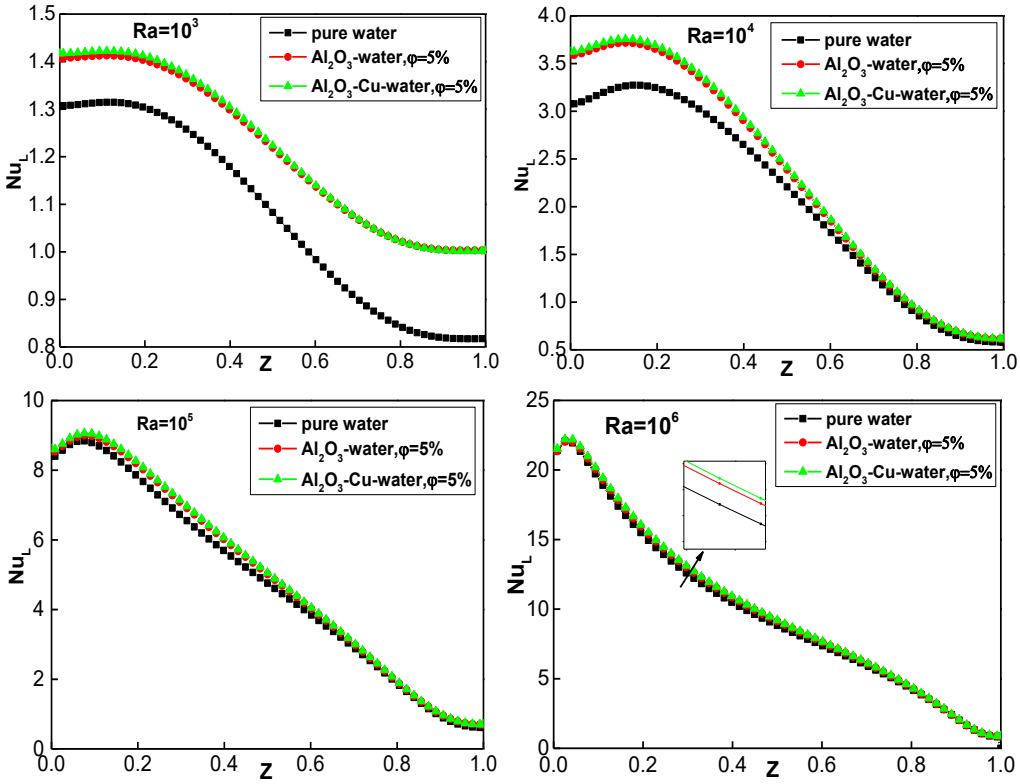

Fig. 9. Nusselt number repartition alongside the heated surface at Y = 0.5 for $\varphi_{hp} = 5\%$.

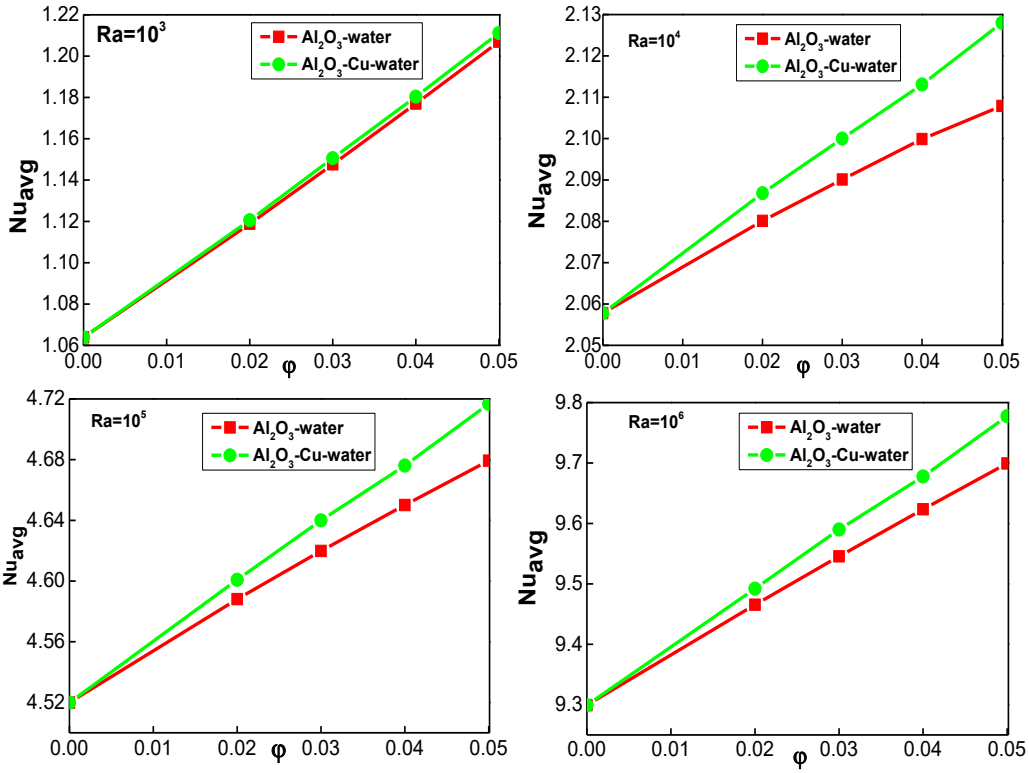

Fig. 10. Evolution of the Nuavg of the nanofluid and the hybrid nanofluid as a function of φ for different numbers of Ra.

The effectiveness of nanoparticles addition on free convection heat transfer enhancement in closed cavities is estimated by increases rate given by:

$$E(\%) = \frac{Nu_{avg,hnf} - Nu_{avg,f}}{Nu_{avg,f}} \times 100 \quad (21)$$

Heat transfer enhancement by adding nanoparticles at various Ra in the case of nanofluid and hybrid nanofluid is shown in Fig. 11. It is shown that E (%) express a similar pattern of increment as indicated by the volume fraction for every single thought about estimation of Ra. In any case, the increase rate obtained for Ra=10^3 is a greater than those determined for Ra=10^4 ; 10^5; 10^6. In later case of higher Rayleigh number, the increase rate is enhanced. However, the impact of the nanoparticles addition is clear when its fraction exceeds 2%.

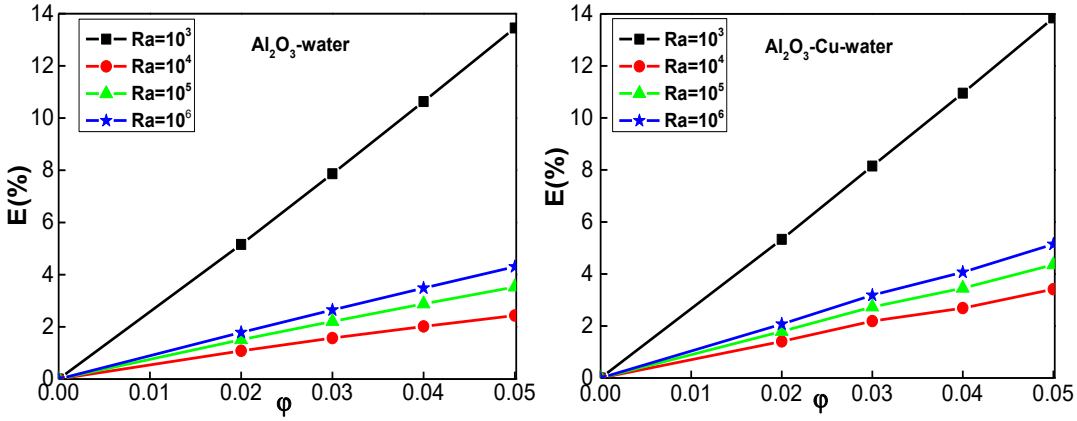

Fig. 11. Evolution of the rate of increase of the Nuavg relative to the volume fraction at ***Ra*** from 10^3 to 10^6 for nanofluid and hybrid nanofluid.

5. Conclusion

In this work, the free convection in heat transfer and fluid flow of water/Al_2O_3 nanofluid and water/Al_2O_3-Cu hybrid nanofluid within three-dimensional cavity was investigated numerically. The finite volume method was chosen to solve the guiding equations.

The effects of various important factors Rayleigh number (10^3-10^6), hybrid volume fraction ($0 \leq \varphi_{hnf} \leq 0.05$) and nanoparticle types on the heat transfer rate as well as the velocity profiles are investigated. The main results found in this paper are as follows:

- The heat transfer is improved with increasing the volume fraction and Rayleigh number.
- The use of hybrid nanofluid provide higher heat transfer in comparison to nanofluid.
- An enhancement of heat transfer is more effectiveness in the case of dominant conduction (low Rayleigh number). However, the increase of the Rayleigh number reverse trend is noticed, in fact, the heat transfer becomes high in the case of dominant heat convection.
- The hybrid nanofluid provide high effect on the Nusselt number at Ra=10^4 Rayleigh number.

The effect of nanoparticles on isotherms is more marked in the case of hybrid nanofluid.

- For similar volume fractions, the average Nusselt number values for the hybrid nanofluid increase up to 1.85% in the case of the Rayleigh number compared to those of the nanofluid

References

[1] Ostrach, S. (1988). Natural convection in enclosures, J. Heat transfer, vol. 10 pp. 1175-1190.

[2] Choi. , U.S. (1995). Enhancing thermal conductivity of fluids with nanoparticules, in:D.A. Siginer, H.P. Wang, (Eds), Developments and applications of non-Newtonian flows, FED-vol.231, 66, pp. 99-105.

[3] Sharif,M.A.R., Mohammend,T.R. (2005).Natural convection in cavities with constant flux heating at the bottom wall and isothermal cooling from the sidewalls, Int. J. Thermal Sciences, vol.44, pp.865-878.

[4] Khanafer, K., Vafai, K, Lightstone, M. (2003). Buoyancy-driven heat transfer enhancement in a two-dimensional enclosure utilizing

nanofluid, Int. J. Heat Mass Transf. 46, 3639-3653.

[5] Oztop, H.F., Dagtekin, I., Bahloul, A. (2005). Comparison of position of a heated thin plate located in cavity for natural convection, Int. Commun. Heat Mass Transfer 32 (2005) 94-106.

[6] Akhter, R., Mokaddes, M. (2022). MHD natural convection in nanofluid filled square cavity with isothermally heated hexagonal block, International Journal of Thermofluid Science and Technology, Vol. 9, pp. 090104.

[7] Saleh,H, Roslan, R., Hashim,(2011). Natural convection heat transfer in a nanofluid-filled trapezoidal enclosure, Int. Heat Mass Transfer 54-194-201.

[8] Tric, E. Labrosse, G., Betrouni, M. (2000). A first incursion into the 3D structure of rnatural convection of air in a differentially heated cubic cavity, from accurate numerical simulations, Int. J.Heat Mass Transfer 43 - 4034-4056.

[9] Ravnik,R., Skerget, L., Hribersek, M. (2010). "Analysis of three-dimensional natural convection of nanofluids by BEM", Engineering Analysis with Boundary Elements, 34 1018-1030.

[10] Ternik, P. (2015). Conduction and convection heat transfer characteristics of water-Au nanofluid in a cubic enclosure with differentially heated sidewalls, Int. J. Heat and Mass Transfer 80-368–375.

[11] Suresh, S., Venkitaraj, K.P., Selvakumar, P. ,Chandrasekar,M.(2012). Effect of Al2O3-Cu/water hybrid nanofluid in heat transfer. Experimental Thermal and Fluid Science, 38:54-60.

[12] Hemmat, M.E., Afrand,M., Yan,Y. ,Yarmand,H, Toghraie, D,Mehidzale. (2016). Effect of temperature and concentration on rheological behavior of MWC-NTs/SiO2 (2080)-SAE40 hybrid nano-lubricants, Int.Commun. Heat Mass Transfer 76- 133-138.

[13] Hemmat, M.E., Arani, A.A., Rezaie, M., Yan, W.M., Karimipour A., (2015). Experimental determination of thermal conductivity and dynamic viscosity of Ag-MgO/water hybrid nanofluid. Int. commun. Heat and Mass Transfer, vol. 66 pp.189-95.

[14] Hemmat, M.E., Sarlak, M.R. (2017). Experimental investigation of switchable behavior of CuO-MWCNT (85% 15%)/10W-40 hybrid nano-lubricants for applications in internal combustion engines, J.Mol.liq.242-326-335

[15] Kalidasan,K., Rajesh P.,K. (2017). Natural convection on an open square cavity containing diagonally placed heaters and adiabatic square block and filled with hybrid nanofluid of nanodiamond cobalt oxide/water, Int.Commun. Heat mass transfer 81 64-71.

[16] Rahman, A.M.R., Leong, K.Y., Azam, C.I, Rashdan, M.S., Anwar M. (2017). Numerical analysis of the forced convective heat transfer on Al2O3-Cu/water hybrid nanofluid, Heat Mass Transf. Vol.53 pp.1835-1842.

[17] Ranga Babu, J.A., Kiran Kumar,K, Srinivasa Rao,S. (2017). State-of-art review on hybrid nanofluids, Renew. Sust. Energ. Rev.77 -551-565.

[18] Aparna, Z., Monisha, M., Pabi, S.K., Ghosh,S . (2019).Thermal conductivity of aqueous Al2O3/Ag hybrid nanofluid at different temperatures and volume concentrations: An experimental investigation and development of new correlation function, Powder Technol.343-714-722.

[19] Mehryan, S.A.M., Kashkooli, F.M., Ghalambaz, M., Chamaka, A.J., (2017). Free convection of hybrid Al2O3-Cu water nanofluid in differentially heated porous cavity, Adv. Powder Technol.28-2295-2305.

[20] Khalili, Z, Sheikholeslami, M., (2023). Investigation of innovative cooling system for photovoltaic solar unit in existence of thermoelectric layer utilizing hybrid nanomaterial and Y-shaped fins, Sustainable Cities and Society .93-104543.

[21] Abu-Nada, E., Oztop H., (2009). "Effect of inclination angle on natural convection in enclosure filled with Cu-water nanofluids", Int. J Heat Fluid Flow, 30-669-678.

[22] Takbi, B. and shokouhmand, H. (2015). Effects of Al2O3-Cu/water hybrid nanofluid on heat transfer and flow characteristics in turbulent regime, Int. J. Modern Physics C Vol.26, No.4 1550047.

[23] Abu-Nada,E, Masoud, Z., Hijazi, A. (2008). Natural Convection Heat Transfer Enhancement in Horizontal concentric annuli Using Nanofluids, Int. Commun. Heat Transfer, Vol. 35, pp. 657-665.

[24] Patankar, S.V. (1980). Numerical Heat Transfer and Fluid Flow, Hemisphere, New York.

[25] Hoffman, J.D. (2001). Numerical Methods for Enginees and Scientists, second ed. Markel Dekker Inc., New York.

[26] Fusegi,T., Hyun,J.M., Kuwahara,K., Farouk,B. (1991). A numerical study of threedimensional natural convection in a differentially heated cubical enclosure, Int. J. Heat Mass Transfer 34 -1543–1557.

[27] Peng,Y., Shu,C., Chew,Y.T., (2003). A 3D incompressible thermal lattice Boltzmann model and its application to simulate natural convection in a cubic cavity, J.Comput. Phys. 193 260–274.

[28] Lo, D.C., Young, D.L. , Murugesan, K. (2005). GDQ method for natural convection in a cubic cavity using velocity–vorticity formulation, Numer. Heat Transfer, Part B 48 – 363–386.

[29] Bajorek, S.M., Lloyed, J.R. (1982). Experimental investigation of natural convection in partitioned enclosures, Journal of Heat Transfer, vol. 104/527.